INTERNATIONAL JOURNAL OF PURE AND APPLIED RESEARCH IN ENGINEERING AND TECHNOLOGY

A PATH FOR HORIZING YOUR INNOVATIVE WORK

A NINE LEVEL CONVERTER TOPOLOGY FOR SINGLE-PHASE TRANSFORMERLESS PV SYSTEM

RASHMI MORE

Dept of Electrical Engineering, GHRIETW, Nagpur-440028.

Accepted Date: 15/03/2016; Published Date: 01/05/2016

Abstract: This paper presents a single-phase transformer less grid connected photovoltaic converter based on two cascaded full bridges with different dc-link voltages. The converter can synthesize upto nine voltage levels with a single dc bus. One full bridge is supplied by a flying capacitor. The multilevel output reduces harmonic distortion and electromagnetic interference. A suitable switching strategy is employed to regulate the flying-capacitor voltage, improve the efficiency and minimize the common-mode leakage current with the help of a novel dedicated circuit (transient circuit). Simulation results confirm the feasibility and good performance of the proposed converter.

Key Words: Multilevel Inverter, Pulse width modulation (PWM), Power switches, Leakage Current, MATLAB software.

Corresponding Author: MS. RASHMI MORE

Access Online On:

www.ijpret.com

How to Cite This Article:

Rashmi More, IJPRET, 2016; Volume 4 (9): 188-200

PAPER-QR CODE

INTRODUCTION

Grid connected photovoltaic converters represent the most widespread solution for residential renewable energy generation. The classical designs of PV converters feature a grid frequency transformer, which is a typically heavy and costly component, at the interface between the converter and the electrical grid, Therefore researchers are now considering transformerless architectures in order to reduce costs and weight and improve efficiency. Removal of the grid frequency transformer overcome all the benefits above but worsens the output power quality, allowing the injection of dc current into the grid and giving rise to the problem of ground leakage current [1].

Although the active parts of photovoltaic modules might be electrically insulated from the ground-connected mounting frame, a path for ac ground leakage currents generally exists due to a parasitic capacitance between the modules and the frame and to the connection between the neutral wire and the ground, usually realized at the low-voltage/medium-voltage (LV/MV) transformer [4]. In addition to deteriorating power quality, the ground leakage current increases the generation of electromagnetic interference and can represent a safety hazard, so that international regulations pose strict limits to its magnitude. This issue must be opposed in all transformerless photovoltaic converters, regardless of architecture. In particular, in full-bridge-based topologies, the ground leakage current is mainly due to high frequency variations of the common-mode voltage at the output of the power converter [5].

Once the grid frequency transformer is removed from a photovoltaic converter, the bulkiest wound and reactive components that remain are those that form the output filter used to clean the output voltage and current from high frequency switching components. Further reduction in cost and weight and improvement in efficiency can be achieved by reducing the filter size, and this is the goal of a multilevel converter.

Multilevel converters have been investigated from years but only recently researches have found their way to commercial photovoltaic converters. Multilevel converters can synthesize the output voltages using more levels, multilevel converters outperform conventional two and three-level converters in terms of harmonic distortion. Moreover, multilevel converters subdivide the input voltage among several power devices, allowing for the use of more efficient devices. Multilevel converters were initially employed in high-voltage industrial and power train applications. They were first introduced in renewable energy converters inside utility-scale plants, in which they are still largely employed. Recently, they have found their way to residential-scale single-phase PV converters, where they currently represent a hot research topic [11].

CFBs give developers many degrees of freedom for the control strategy. A CFB made up of *n* full bridges and at least 4*n* power switches can synthesize 2*n* + 1 voltage levels when the supply voltage is the same for each full bridge. Reduction in the switches per output voltage- level ratio can be achieved in CFB structures if different supply voltages are chosen for each full bridge.

The topology proposed in this paper consists of two symmetrical CFBs, generating nine output voltage levels. In the proposed converter, the dc voltage source supplies one of the full bridges and a flying capacitor supplies the other one. By suitably controlling the ratio between the two voltages, different sets of output levels can be obtained.

The flying capacitor used as a secondary energy source which allows limited voltage boosting. The number of output levels per switch (eight switches, nine levels) is comparable with what can be achieved using custom architectures. In final topology two additional very low power switches and a line frequency switching device [transient circuit (TC)] were included in order to reduce the ground leakage current. It is important to put in evidence that the proposed converter can work at any power factor as reported in Section III.

This paper is organized as follows: Section II presents the power converter topology and the PWM control strategy. Section III describes the regulation of the flying capacitor used to supply the second full bridge of the CFB topology. Section IV describes the principle of operation of the additional components able to reduce the ground leakage current. Sections V and VI show the Matlab design and simulation results, whereas Section VII reports the concluding remarks.

II. NINE-LEVEL CONVERTER AND PWM CONTROL STRATEGY

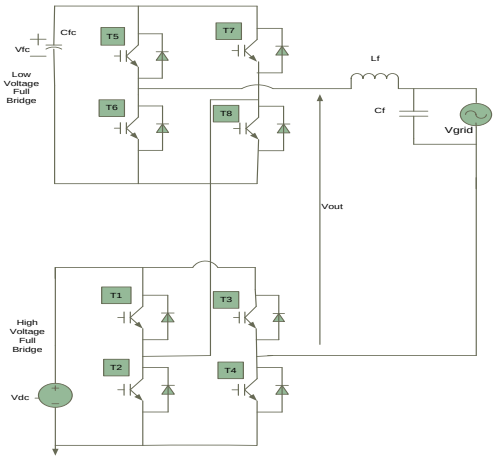

Fig. 1. CFB with a flying capacitor.

The proposed converter is composed of two CFBs, one bridge is supplied by a flying capacitor (Fig. 1). The PWM strategy alone is not sufficient to maintain a low ground leakage current, other components were added as described in Section IV. The proposed PWM strategy stretches the efficiency by using the two legs where PWM frequency switching does not occur. Insulated-gate bipolar transistors (IGBTs) with fast antiparallel diodes are required in the legs where high-frequency hard-switching commutations occur. In Grid-connected operation, one full-bridge leg is directly connected to the grid neutral wire, whereas the phase wire is connected to the converter through an *LC* filter. Flying-capacitor voltage *Vfc* is kept lower at steady state than dc-link voltage V_{DC}. Accordingly, the full bridge supplied by the dc link is called the high-voltage full bridge (HVFB) and one with the flying capacitor is the low-voltage full-bridge (LVFB).

The CFB topology allows certain degrees of freedom in the control, so that different PWM schemes can be considered however, the chosen solution needs to satisfy the following requirements.

1) Most commutations must take place in the LVFB to limit the switching losses.

2) The neutral-connected leg of the HVFB needs to switch at load frequency to reduce the ground leakage current.

3) The redundant states of the converter must be properly used to control the flying-capacitor voltage.

TABLE I DESCRIPTION OF THE CONVERTER OPERATING ZONES

Zone	Output Voltage	On Devices	Off Devices	Switching Devices
Zone3B	$-V_{DC} - V_{FC} \leftrightarrow -V_{DC}$	T2, T3,T7	T1, T4, T8	T5, T6
Zone3A	$-V_{DC} \leftrightarrow -V_{DC}+V_{FC}$	T2, T3,T8	T1, T4, T7	T5, T6
Zone2A	$-V_{DC} + V_{FC} \leftrightarrow 0$	T3, T7	T4, T8	T1, T2, T5,T6
Zone2B	$-V_{DC} \leftrightarrow -V_{FC}$	T3, T7	T4, T8	T1, T2, T5,T6
Zone1B	$-V_{FC} \leftrightarrow 0$	T1, T3,T7	T2, T4, T8	T5, T6
Zone1A	$0 \leftrightarrow V_{FC}$	T2, T4,T8	T1, T3, T7	T5, T6
Zone2A	$V_{FC} \leftrightarrow V_{DC}$	T4, T8	T3, T7	T1, T2, T5,T6
Zone2B	$0 \leftrightarrow V_{DC} - V_{FC}$	T4, T7	T3, T7	T1, T2, T5,T6
Zone3B	$V_{DC} - V_{FC} \leftrightarrow V_{DC}$	T1, T4,T7	T2, T3, T8	T5, T6
Zone3A	$V_{DC} \leftrightarrow V_{DC} + V_{FC}$	T1, T4,T8	T2, T3, T7	T5, T6

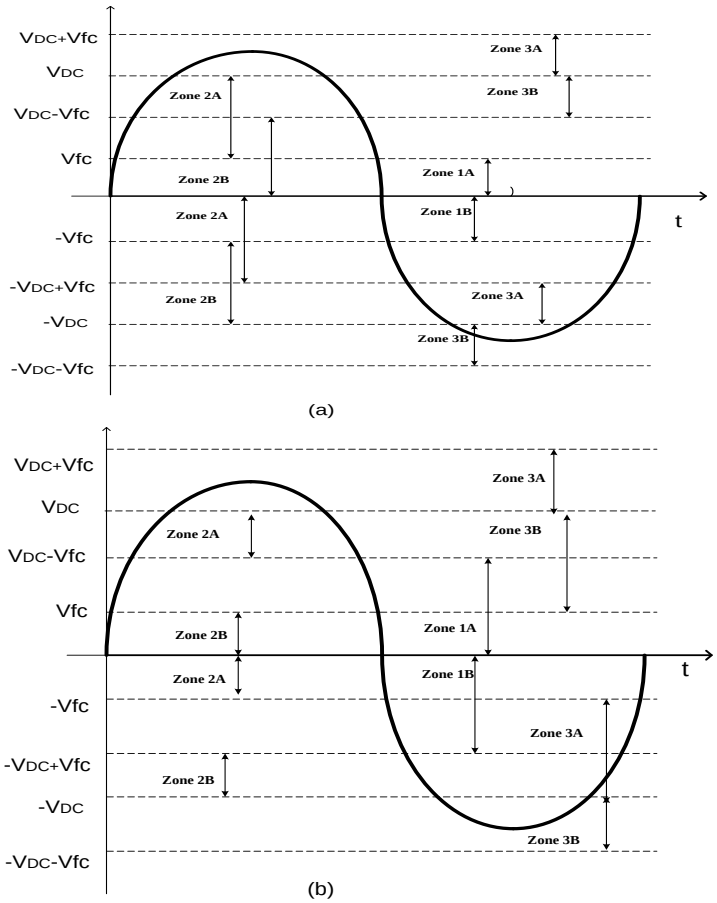

Fig. 2. Operating zones under different *Vfc* ranges. (a) *V*fc < 0.5*VDC*. (b) *V*fc > 0.5*VDC*.

The switching pattern described in Table I was developed according to the above requirements. Capacitive coupling makes the common-mode current inversely proportional to the switching frequency of the neutral-connected leg.

The converter can operate in different output voltage zones, where the output voltage switches between two specific levels. The operating zone boundaries vary according to the dc-link and flying-capacitor voltage and adjacent zones can overlap (Fig. 2).

In A zones the contribution of the flying-capacitor voltage to the converter output voltage is positive, whereas it is negative in B zones. Constructive cascading of the two full bridges result in limited output voltage boosting. Depending on the V_{fc}/V_{DC} ratio, one of the (a) or (b) situations in Fig. 2 can ensure the operation of the converter. It does not differ much in the two cases. If two overlapping operating zones can supply the same output voltage, the operating zone to be used is determined taking into account the regulation of V_{fc}, as will be described in Section III.

The switching pattern depends on the instantaneous fundamental component of output voltage *Vout* and on the measured values of V_{fc} and V_{dc}. If $V_{fc} = V_{DC}/3$, the converter can synthesize nine equally spaced output voltage levels. One leg of the HVFB operates at grid frequency and one leg of the LVFB at five times the grid frequency.
Apart from zone 2, no high-frequency commutations occur in the whole HVFB (Fig. 2). Since the voltage regulation of the flying capacitor takes place in zone 2, the zone-2 behavior is more articulated and will be described in detail in the following section.

III. FLYING-CAPACITOR VOLTAGE REGULATION

Main task facing a Grid-connected photovoltaic converter is the transfer of active power to the electrical grid because controlling the voltage of the flying capacitor is critical.
Flying-capacitor voltage V_{fc} is regulated by suitably choosing the operating zone of the converter depending on the instantaneous output voltage request. Depending on the operating zone of the converter (Fig. 2), $_{Vfc}$ can be added to (A zones) or subtracted from (B zones) the HVFB output voltage, charging or discharging the flying capacitor. In particular, considering a positive value of the current injected into the grid, the flying capacitor is discharged in A zones and charged in B zones. Since a number of redundant switch configurations can be used to synthesize the same output voltage waveform, it is possible to control the voltage of the flying capacitor, forcing the converter to operate more in A zones when the flying-capacitor voltage is higher than a reference value or more in B zones when it is lower than a reference value. Similar considerations hold in case of a negative injected current.

In each case, some commutations between nonadjacent output levels must inevitably occur (level skipping), with the drawback of a certain increase in the output current ripple. The voltage control of the flying capacitor (which determines the zone-A or zone-B operation) is realized by a simple hysteresis control.

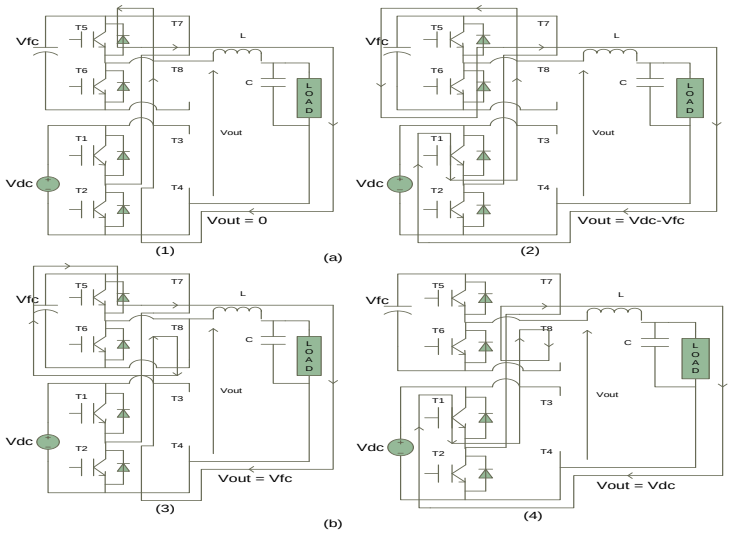

Fig. 3. Converter configurations for the regulation of the flying capacitor. (a) Flying-capacitor charge. (b) Flying-capacitor discharge.

Fig.3. illustrates the regulation of *V*fc supposing a positive current with *V*out > 0 and *V*fc < 0.5V_{DC}. If *V*fc is too low, output level *V*fc can be replaced by V_{DC} − *V*fc, thus switching between the 0 and V_{DC} − *V*fc output levels [zone 2B, Fig.3(a)]. Similarly, if *V*fc is too high, V_{DC}–*V*fc can be replaced with *V*fc, causing the converter to switch between the *V*fc and V_{DC} output level[zone 2A, Fig.3(b)]. In Fig. 3, the devices switching at low frequency are short circuited when on and not shown when off. Similar *V*fc regulation strategies can be likewise developed for the case when *V*fc > 0.5V_{DC}.

If *V*fc < 0.5V_{DC}, in order to minimize the current ripple,

zone 2 is chosen only when *V*fc < *V*out < V_{DC}–*V*fc (zones 3 are otherwise chosen), limiting level skipping. Level skipping always occurs if *V*fc > 0.5V_{DC} hence, any A or B zone can be chosen according to the voltage regulation algorithm.

Since the dc-link voltage can go through sudden variations due to the MPPT strategy, it is important that the converter is able to work in any [V_{DC}, *V*fc] condition. While the distortion of the output voltage is minimized through the on-line duty cycle computation, it is important to assess the capability of the converter to regulate the flying-capacitor voltage under different operating conditions.

IV. APPLICATION TO TRANSFORMERLESS

PV CONVERTERS—TC

A particular feature of the commutation pattern of Table I is that T3 and T4 switches at grid frequency, commutating at every zero crossing of *V*grid. If the zero crossing with a negative

derivative is considered, T4 opens and T3 closes, changing the neutral wire voltage (and thus the voltage across the parasitic capacitance of the PV field) from zero to V_{DC}. For this reason, the commutation can cause a large surge of leakage current that can decrease the power quality and damage the photovoltaic modules. A proper TC was designed to decrease these surge currents.

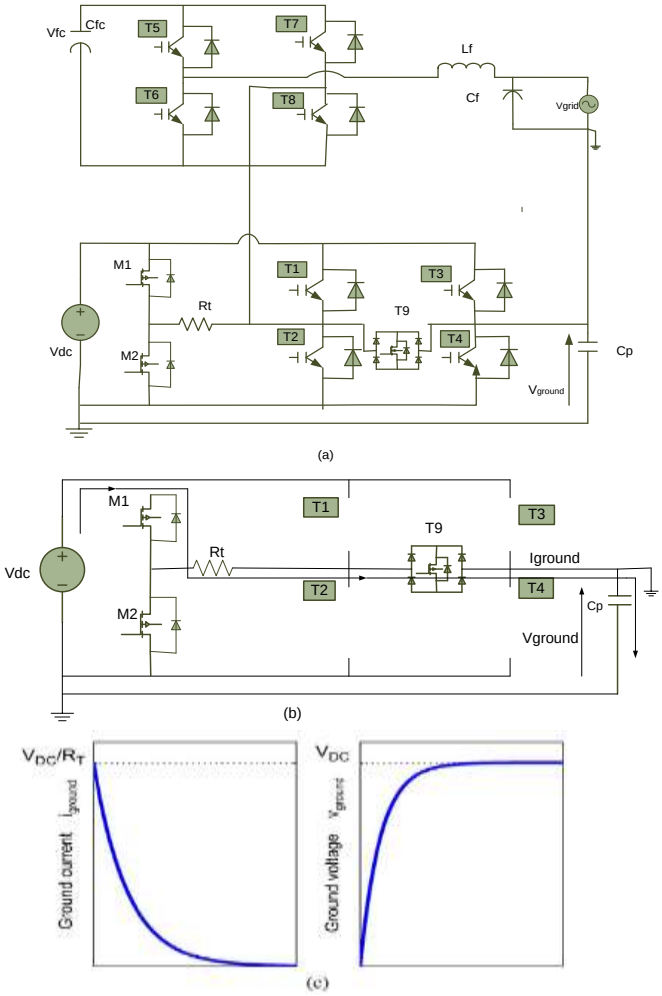

Fig. 4. Ground leakage current limitation circuit topology and behavior.
(a) TC topology. (b) TC operation. (c) TC waveforms.

Fig. 4(a) shows the proposed converter topology, it is constituted of the two-cell CFB described in Fig. 1 with the addition of the TC components. In order to better understand the behavior of the TC, the distributed parasitic capacitance of the PV source was modeled with a simple

equivalent parasitic capacitance i.e. *Cp*, connected between the negative pole of the dc link and the ground.

The TC consists of two low-power MOSFETs M1 and M2, bidirectional switch T9, and resistor R_T. When the converter enters operating zone 1, the HVFB output voltage must be zero which is obtained by switching T1 and T3 or T2 and T4 on. To operate the TC, when entering zone 1, T1, T2, T3, and T4 are all kept off, while T9 is on. This keeps the neutral potential floating, so that the voltage on the parasitic capacitor Vground remains constant [see Fig. 4(b)]. At this point, one of M1 and M2 is turned on (M1 if the slope of the zero crossing is negative and M2 if positive). So *Cp* is charged through R_T with a first-order transient [see Fig. 4(c)], limiting the current surge.

Whereas the TC introduces additional components, they can be selected with current ratings much lower than the devices of the CFB. Moreover, the power loss due to the added resistor is negligible. Calulating the energy lost charging and discharging a capacitor *Cp* to V_{DC} averaged over a line period *T* by $P\text{tc} = CpV^2_{DC}/T$, with *Cp* = 200 nF and V_{DC} = 300 V, a dissipation of about 1W is obtained. The operation of the TC is not affected by the power factor because in Grid-connected operation, the output voltage is always very close to the Grid voltage.

V. MATLAB DEGIGN CIRCUIT

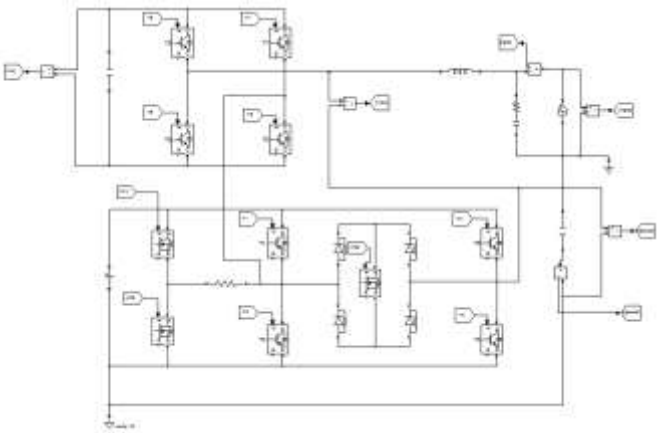

Fig. 5. Matlab design circuit for nine level converter topology.

VI. SIMULATION RESULTS

The proposed converter and PWM were extensively simulated under MATLAB/Simulink. The simulations cover a large range of active and reactive power injected into the grid, dc-link voltage, and equivalent PV parasitic capacitance. A dc-link voltage V_{DC} = 300 V was used in the simulations. The grid was represented by a sinusoidal voltage source at 50 Hz of amplitude

*V*grid = 230 V. The output filter was composed of a capacitor *Cf* = 1 μF and an inductor *Lf* = 1.5 mH.

The PWM frequency was *fs* = 20 kHz, and the flying capacitor had a capacitance of *C*fc = 500 μF. The surge limiting resistance *RT* was selected as 1.5 kΩ. The current injected into the grid was regulated through a proportional-integral regulator plus feedforward at *i*grid = 8.5 A rms.

As stated above, the injection of both active and reactive power was simulated however, the switches being ideal and the commutations instantaneous, performance did not depend on the power factor. For this reason, only the unity power factor simulation results are reported in the simulation.

Fig. 6 shows the output voltage and curren. As expected, the THD of the grid current is 2.7%.

Fig. 7 shows the performance of the TC with a parasitic capacitance of the PV field of *Cp* = 200 nF. The ground leakage current results *i*ground = 30 mA rms. The ground leakage current could be further reduced by a more accurate design of the common-mode filter.

Fig. 8 reports flying capacitor voltage. Variation of *V*fc from 90 to 110 V occurring at time 0.1 s. As it can be seen, the average value of *V*fc rapidly (in about 25 ms) rises to the reference value without any overshoot.

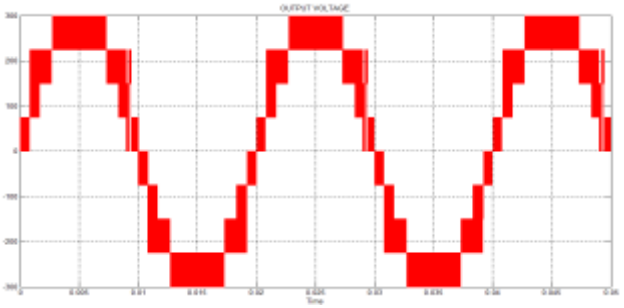

(a)

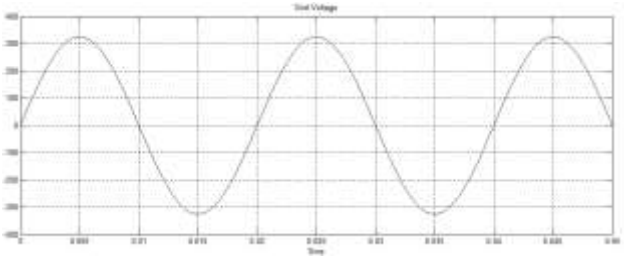

(b)

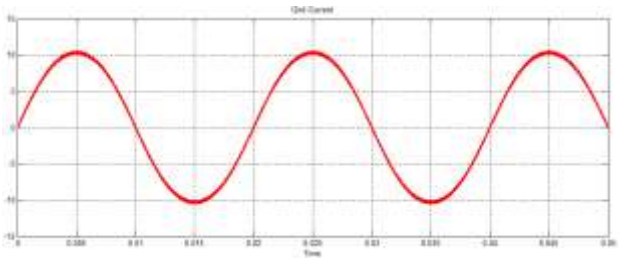

(c)

Fig. 6. Simulation results with VDC = 300 V (a) Inverter output voltage waveform. (b) Grid Voltage waveform. (c) Grid Current waveform.

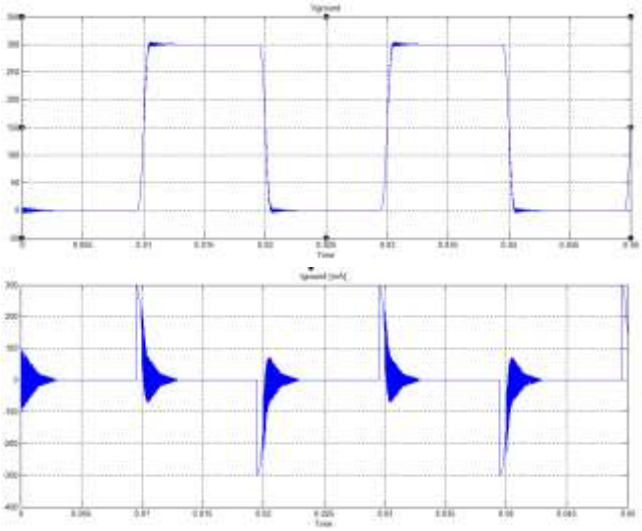

Fig. 7. TC behavior with a 200 nF parasitic capacitor.

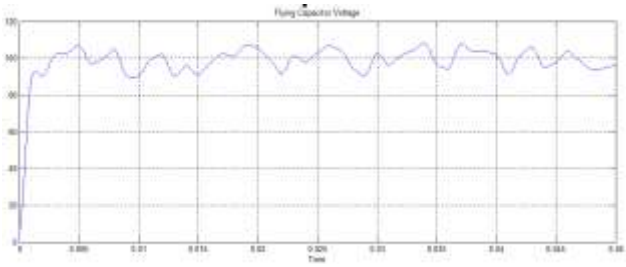

Fig. 8. Flying capacitor voltage.

V. CONCLUSION

This paper has proposed a novel nine-level converter topology for transformer less PV converter based on a CFB topology with two full bridges, one of which is supplied by a floating capacitor.

A suitable PWM strategy was developed in order to improve efficiency and with the help of a specific TC, minimize the ground leakage current.

The proposed PWM strategy can regulate the voltage across the flying capacitor. Simulation was performed to assess the ability to regulate the flying-capacitor voltage in a wide range of operating conditions.

The proposed converter can continuously operate at arbitrary power factors, has limited boosting capability, and can produce nine output voltage levels with 11 power switches, of which three are low power switches for the TC and only four need to be controlled by PWM.

REFERENCES

1. G. Buticchi, Davide Barater, Emilio Lorenzani, Carlo Concari "A Nine-Level Grid-Connected Converter Topology for Single-Phase Transformerless PV Systems" , *IEEE Trans. Ind. Electron.*, Vol, 61, No. 8, Aug. 2014

2. G. Buticchi, L. Consolini, and E. Lorenzani, "Active filter for the removal of the dc current component for single-phase power lines," *IEEE Trans. Ind. Electron.*, vol. 60, no. 10, pp. 4403–4414, Oct. 2013

3. G. Buticchi and E. Lorenzani, "Detection method of the dc bias in distribution power transformers," *IEEE Trans. Ind. Electron.*, vol. 60, no. 8, pp. 3539–3549, Aug. 2013.

4. H. Xiao and S. Xie, "Leakage current analytical model and application in single-phase transformerless photovoltaic Grid-connected inverter," *IEEE Trans. Electromagn. Compat.*, vol. 52, no. 4, pp. 902–913, Nov. 2010

5. O. Lopez, F. Freijedo, A. Yepes, P. Fernandez-Comesaa, J. Malvar, R. Teodorescu, and J. Doval-Gandoy, "Eliminating ground current in a transformerless photovoltaic application," *IEEE Trans. Energy Convers.*, vol. 25, no. 1, pp. 140–147, Mar. 2010.

6. S. Araujo, P. Zacharias, and R. Mallwitz, "Highly efficient single-phase transformer less inverters for Grid-connected photovoltaic systems," *IEEE Trans. Ind. Electron.*, vol. 57, no. 9, pp. 3118–3128, Sep. 2010.

7. D. Barater, G. Buticchi, A. Crinto, G. Franceschini, and E. Lorenzani, "Unipolar PWM strategy for transformerless PV Grid-connected converters," *IEEE Trans. Energy Convers.*, vol. 27, no. 4, pp. 835–843, Dec. 2012.

8. T. Kerekes, R. Teodorescu, P. Rodridguez, G. Vazquez, and E. Aldabas, "A new high-efficiency single-phase transformerless PV inverter topology," *IEEE Trans. Ind. Electron.*, vol. 58, no. 1, pp. 184–191, Jan. 2011.

9. S. Kouro, M. Malinowski, K. Gopakumar, J. Pou, L. Franquelo, B. Wu, J. Rodriguez, M. P. Andrez, and J. Leon, "Recent advances and industrial applications of multilevel converters," *IEEE Trans. Ind. Electron.*, vol. 57, no. 8, pp. 2553–2580, Aug. 2010.

10. Mohammad Kazem Bakhshizadeh, Hossein Iman-Eini, Frede Blaabjerg "Selective Harmonic Elimination in Asymmetric Cascaded Multilevel Inverters Using a New Low-frequency Strategy for Photovoltaic Applications" *Electric Power Components and Systems*, Doi: 10.1080/15325008.2015.1021058

11. G. Buticchi, E. Lorenzani, and G. Franceschini, "A five-level single-phase Grid-connected converter for renewable distributed systems," *IEEE Trans. Ind. Electron.*, vol. 60, no. 3, pp. 906–918, Mar. 2013

12. J. Chavarria, D. Biel, F. Guinjoan, C. Meza, and J. Negroni, "Energy balance control of PV cascaded multilevel Grid-connected inverters under level-shifted and phase-shifted PWMS," *IEEE Trans. Ind. Electron.*, vol. 60, no. 1, pp. 98–111, Jan. 2013.

13. G. Grandi, C. Rossi, D. Ostojic, and D. Casadei, "A new multilevel conversion structure for Grid-connected PV applications," *IEEE Trans. Ind. Electron.*, vol. 56, no. 11, pp. 4416–4426, Nov. 2009.S. Daher, J. Schmid, and F. Antunes, "Multilevel inverter topologies for stand-alone PV systems," *IEEE Trans. Ind. Electron.*, vol. 55, no. 7,pp. 2703–2712, Jul. 2008.

14. S. Daher, J. Schmid, and F. Antunes, "Multilevel inverter topologies for stand-alone PV systems," *IEEE Trans. Ind. Electron.*, vol. 55, no. 7,pp. 2703–2712, Jul. 2008.